CrossMark

Three-dimensional direct laser written graphitic electrical contacts to randomly distributed components

Bryce Dorin[1,2] · Patrick Parkinson[1,3] · Patricia Scully[1,2]

Abstract

The development of cost-effective electrical packaging for randomly distributed micro/nano-scale devices is a widely recognized challenge for fabrication technologies. Three-dimensional direct laser writing (DLW) has been proposed as a solution to this challenge, and has enabled the creation of rapid and low resistance graphitic wires within commercial polyimide substrates. In this work, we utilize the DLW technique to electrically contact three fully encapsulated and randomly positioned light-emitting diodes (LEDs) in a one-step process. The resolution of the contacts is in the order of $20\,\mu m$, with an average circuit resistance of $29 \pm 18\,k\Omega$ per LED contacted. The speed and simplicity of this technique is promising to meet the needs of future microelectronics and device packaging.

1 Introduction

The drive towards device miniaturization has led to a surge in the development of micro/nano-scale electronics. Many complex electrical components, such as nanowires, can be grown epitaxially on crystal substrates with sub-micron dimensions [1–5]. To package these components economically into functional devices, one must fabricate inexpensive and reliable electrical contacts to them. This step often becomes a significant challenge as the small size and random distribution of the devices are incompatible with standard metallization techniques [6]. Printed circuit boards (PCBs) and reflow soldering are effective tools for mounting and contacting electrical components, but are limited by fixed PCB layouts and relatively large feature sizes ($> 50\,\mu m$). In a laboratory setting, techniques such as electron beam lithography and beam-assisted chemical vapour deposition are able to fabricate sufficiently small electrical contacts [7],

however, the complexity and cost of these methods prevents them from being economical in an industrial setting.

In recent work, our group has demonstrated the ability to electrically contact encapsulated and randomly distributed silver nanowires using a three-dimensional (3D) direct laser writing (DLW) process [8]. This demonstration was significant as it introduced a novel method for rapidly creating 3D electrical circuits encapsulated within an insulating polymer using a single processing step. During this DLW process, the bulk of polyimide (PI) is converted to graphite at the laser focus, which becomes 16 orders of magnitude more conductive than virgin PI. A similar technology has also been demonstrated using advances in ink-jet printing [9], however, these 3D conductive circuits are not formed within an encapsulant. In this work, the term "encapsulated" is defined to mean sealed (at least in part) from ambient conditions.

PI is a chemically and thermally stable polymer used in a variety of insulating applications. It was discovered in 1991 that after exposure to laser irradiation, PI is converted into conductive graphite through a thermochemical process [10, 11]. It has been proposed that during this process the C=O, C-O, C-N bonds in the PI are ruptured, producing CO, HCN and C_2H_2 gases [12, 13]. What remains encapsulated in the PI is a conductive network of graphitic nanocrystals. Following this discovery, it was reported that porous graphene networks can also be created using a DLW technique, which led to the development of DLW capacitors [14–16] and sensors [17].

✉ Bryce Dorin
  bryce.dorin@manchester.ac.uk

1 The Photon Science Institute, The University of Manchester, Oxford Road, Manchester M13 9PL, UK

2 School of Chemical Engineering and Analytical Science, The University of Manchester, Oxford Road, Manchester M13 9PL, UK

3 School of Physics and Astronomy, The University of Manchester, Oxford Road, Manchester M13 9PL, UK

Until recently, structures created in PI through DLW were fabricated only on the surface using continuous-wave laser sources, limiting the devices to two dimensions. However, our group has now exploited the non-linear absorption of femtosecond pulses in PI to generate graphitic wires in 3D [8]. This discovery enabled the fabrication of electrical contacts to fully encapsulated structures. A similar technique was also developed concurrently and independently by Wang and colleagues for the manufacture of stacked capacitors in PI [18].

Building on our previous work, we demonstrate the ability of DLW in PI to form electrical contacts to a series of three randomly distributed micro-scale light-emitting diodes (μLEDs) encapsulated in a clear epoxy. Through this, we establish DLW in PI as a practical methodology for electrical contacting useful devices with negligible contact impedances. We also make use of Raman spectroscopy, scanning electron beam microscopy (SEM), and energy dispersive X-ray spectroscopy (EDS) to further characterize the laser-modified regions of the PI. The results of these measurements give us further insight into the chemistry of the DLW process, as well as the structure of the graphitic product.

2 Experimental

A Coherent RegA Ti:Sapphire system with an output wavelength centred at 800 nm and a repetition rate of 100 kHz was used as the laser source for the DLW described in this work. A linear polarization was also maintained during all experiments. The minimum duration of the output pulses ranged from 150–180 fs, which was monitored using an autocorrelator (assuming a $sech^2$ pulse shape). Laser pulse energy at the sample was varied 0.5–1.0 μJ using a diffractive optical attenuator. The laser beam was focused in the sample to a spot size of 2.5 μm through a 0.45 NA objective. Under these experimental conditions, the calculated power intensity at the focus ranged from $7 \times 10^{13} - 1.4 \times 10^{14}$ W/cm^{-2}. The scan speed during writing was determined by the speed of the three-axis stage (Aerotech ANT130) that mounted the samples.

The experimental samples were prepared as follows. Kapton^ HN sheets 127 μm thick, supplied by DuPont^{TM}, were used as the PI substrates. These sheets were washed with isopropyl alcohol before use. Using tweezers, orange μLEDs supplied by Kingbright (part number: KPHHS-1005SECK) were randomly placed on the PI substrates with their electrodes touching the PI surface. The μLEDs were then encapsulated in ~ 1 mm of clear epoxy (Opti-tec^{TM} OPT 5012). After fabricating the electrical contacts through PI to the μLEDs using DLW, silver paint (Alfa Aesar 45661) was used to create low impedance contacts between the DLW regions and gold electrical probes. Current-voltage (IV)

measurements were then performed using a Keithley 487 Picoammeter.

Further analysis of the DLW regions was carried out through optical microscopy, Raman spectroscopy, environmental SEM imaging, and EDS. The use of an environmental SEM allows imaging of the samples under low pressure, avoiding the requirement for conductive coatings. EDS data was also collected during SEM imaging. The Raman spectroscopy was performed using a Renishaw 1000 Raman microscope, with 2.32 mW of power at a 514 nm wavelength focused on the sample using a 0.55 NA objective.

3 Results and discussion

Initial experiments involved contacting single μLEDs using DLW contacts to the anodes and cathodes of the devices. In Fig. 1a, a schematic is provided that illustrates the configuration of a μLED and the DLW contacts. To reach the fully encapsulated μLEDs, contacts were fabricated through the PI in the form of *vias*. These *vias* are inscribed by positioning the focus of the laser at the interface between the μLED electrodes and the PI substrate, then scanning the focus through the bulk of the PI to its surface. The pulse energy was set to 0.5 μJ to avoid ablation at the surface of the PI. The scan rate was 10 000 pulses μm, which was previously determined to be the optimal speed for creating low resistivity *vias* [8]. After DLW, a turn-on procedure was performed, which uses Joule heating to anneal the *vias* into a high conductivity state, as described by previous work [8]. The μLEDs did not exhibit any degradation during this turn-on process. Five μLEDs were contacted through this method, all of which demonstrated a measurable conductivity and emitted light. The IV data for these five devices is shown in Fig. 1b, where the average resistance of the circuits is 29 ± 18 kΩ. The resistance of the μLEDs themselves contributes negligibly to this value when biased above their voltage threshold. The diode voltage threshold was found to be 1.8 ± 0.1 V, which agrees with the information quoted in the technical data sheet for the μLEDs [19].

In Fig. 2 we analyze a cross-section of a through-PI-*via* to further understand the DLW process. Optical microscope and SEM images are provided in Fig. 2a, b, respectively. It can be seen that the optical image provides the best picture of the *via*, as the SEM image lacks contrast between irradiated and non-irradiated regions. From these images, we note that the *via* forms a consistent cylindrical shape through the PI, with very little ablation at the front or back surfaces.

EDS spectra were collected at five locations along the *via* and on the virgin PI. From the raw EDS data, the strength of the oxygen signal was divided by the strength of the carbon signal, which is plotted in Fig. 2c. This ratio provides a metric for determining if oxygen is being ejected from
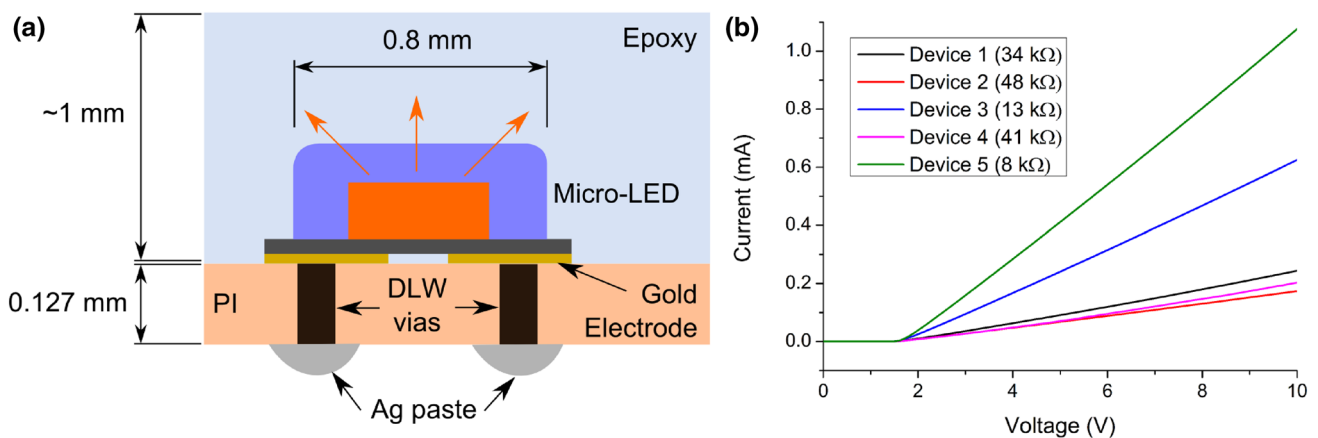
Fig. 1 Contact to a single µLED using DLW. In **a** a schematic demonstrates the µLED encapsulation and the DLW contacts that are fabricated. In **b** IV measurements are provided for five contacted µLED devices
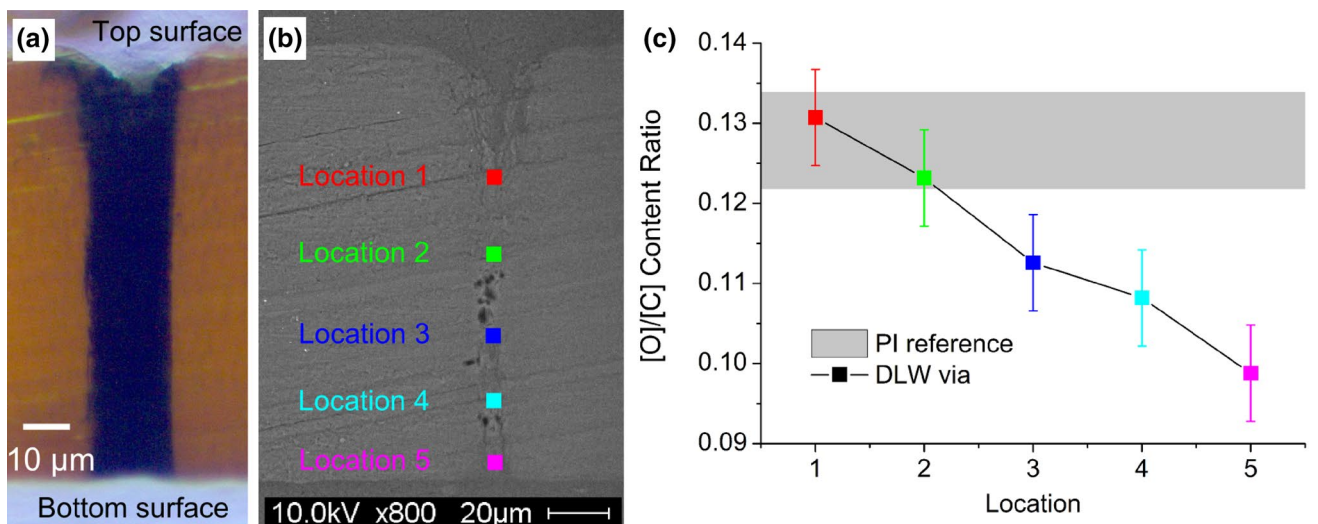

Fig. 2 Analysis of a DLW *via* through PI. Images **a** and **b** are optical microscope and SEM images of the *via*, respectively. The plot in **c** displays EDS data from the points marked in image **b**. Here, the ratio of oxygen to carbon content at each point is compared to that of virgin PI

the PI in gaseous form during the DLW process. As a reference, we used the [O]/[C] value for virgin PI. From this data, one can see that the oxygen content along the DLW *via* is lowest closest to the back surface of the PI. At the front surface the ratio matched that of virgin PI within error. This result is surprising as the exact same DLW process was applied to the entire length of the *via*. However, one explanation could be that the gases produced in the *via* require a DLW pathway through the PI to escape. The DLW process begins at the back surface, therefore, diffusion of the gases to the ambient environment is easiest when formed nearer the back surface. As DLW progresses further towards the front surface, the gases produced, which are still unable to escape from the front surface, are less likely to diffuse to the back surface and are, therefore, trapped inside the *via*. One

question that emerges from these results is if conductivity also varies along the length of the *via*, which is the subject of future work.

Comparing the device resistances measured in Fig. 1b to that of the individual *vias* measured previously ($16 \pm 5\,\text{k}\Omega$) [8], we find that the resistance of the contacted µLEDs can be accounted for by the *vias* themselves well within error. This indicates that the contact resistance between the µLEDs and DLW *vias* is negligible within error. This is an exciting discovery as it was found that when contacting silver nanowires, contact resistance is the dominate source of resistance in the circuit. It is believed this high contact resistance is due to the very small contact area available on nanowires, which is not the case for the µLEDs. The relatively high resistance variability observed in the devices of Fig. 1b is consistent

with the resistance variability measured in individual vias in [8]. Raman spectroscopy measurements of a via cross-section performed in [8] suggest this high resistance variability may arise due to the presence of graphitic nanocrystals in an amorphous carbon network.

For a typical contacted μLED device, the PI and epoxy layers were carefully removed from each other, allowing us to study the nature of the contact formed between the *via* and the μLED electrodes. A microscope image of this contact is shown in Fig 3a. It can be seen that a black substance has adhered to the contact at the location of the via. Fig. 3b plots the results of Raman spectroscopy on the black substance. Two clear peaks emerge in this sample, which closely match the peaks, the D and G peaks

associated with graphitic carbon [20]. We, therefore, conclude that the source of the low contact resistance between the *vias* and μLEDs is this adhesion of the DLW graphite to the electrode.

The potential of this micro-fabrication technique is demonstrated in Fig. 4, which presents a DLW circuit containing three randomly distributed μLEDs connected in series. Each μLED was contacted by a *via* at the anode and cathode. The vias were then interconnected by wires laser written on the surface of the PI using 1.0 μJ/pulse and 20 pulses/μm. An image of the three interconnected μLEDs viewed from the back (PI) surface is shown in Fig. 4a. Fig. 4b is an image of the front (epoxy) surface of the device, where one can see all three μLEDs are turned-on under a 10 V bias. The IV data
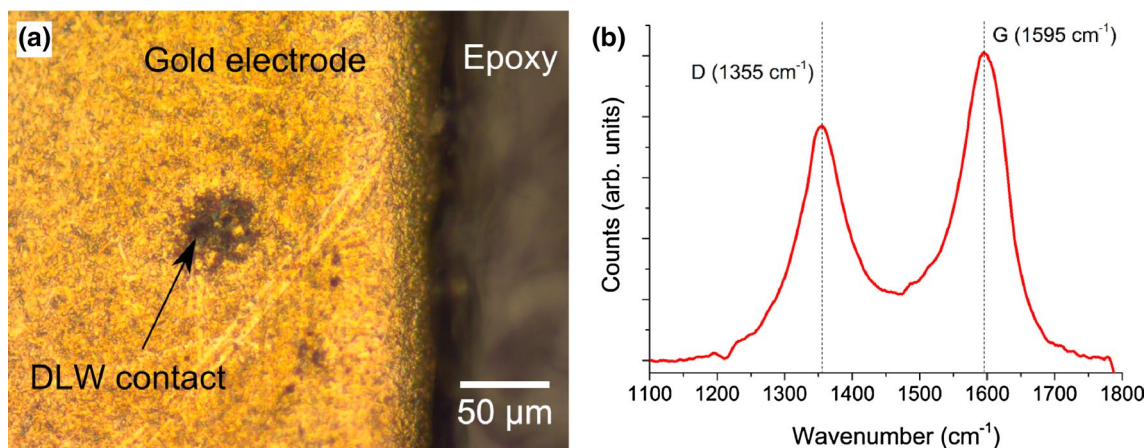

Fig. 3 An investigation into the contact between the DLW *vias* and the μLED electrodes. The image in **a** demonstrates the formation of a black substance on the gold electrodes of the μLEDs after DLW. The Raman spectrum in **b** confirms this substance is graphite produced during DLW that adhered to the surface of the electrodes
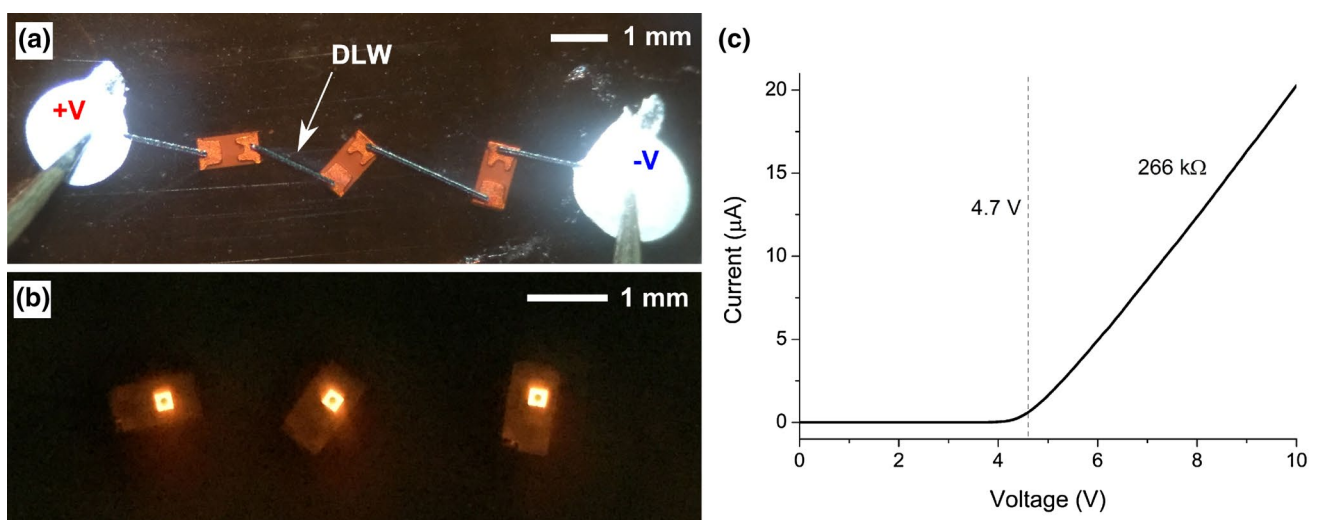

Fig. 4 The contact of three μLEDs in series. The images in **a** and **b** show the configuration of the μLEDs and the DLW contacts viewed from the back and front surfaces, respectively. In **c** the IV data for the circuit is displayed

for this device is provided in Fig. 4c. The total resistance of the system is $266\,k\Omega$.

Separate experiments were carried out to determine the sources of resistance in the device depicted in Fig. 4. Based on our previous results, we expect the six *vias* to account for $\sim 1/3$ of this total resistance. The DLW graphitic wires on the surface of the PI have a relatively low resistance ($\sim 2\Omega/mm$), therefore, contribute little to the total resistance of the circuit. The largest source of resistance in the circuit is most likely the contact between DLW surface wires and *vias*, which experimental measurements indicate can range from 1 to $85\,k\Omega$. In future work, decreasing the resistivity of this component will be key to improving the overall performance of the device.

4 Conclusions

In this work, we demonstrate an application for 3D electrical circuits encapsulated within PI, which are fabricated using a one-step DLW process. Three fully encapsulated and randomly distributed μLEDs were electrically contacted in series, producing a functional device. The contact resistance measured in this work has improved significantly compared to previous efforts [8]. Through Raman spectroscopy, we observe graphite adhering well to the gold electrodes of the μLEDs. We have also investigated the distribution of elements within the DLW *vias* using EDS. It was observed that the oxygen content varied along the length of the *via*. This distribution may correspond to the ability of oxygen-containing gases to diffuse along the DLW pathway to the surface of the PI. From a commercial perspective, this work contains promising demonstrations of electrical packaging for the next generation of micro/nano-scale components. The capability of this technique to electrically contact randomly positioned devices that are fully encapsulated from the environment is not available using any other methodology.

References

1. P. Parkinson, Y.H. Lee, L. Fu, S. Breuer, H.H. Tan, C. Jagadish, Nano Lett. **13**, 1405–1409 (2013)
2. R. Yang, Y. Qin, L. Dai, Z.L. Wang, Nat. Nanotechnol. **4**, 34–39 (2009)
3. Y. Dong, G. Yu, M.C. McAlpine, W. Lu, C.M. Lieber, Nano Lett. **8**(2), 386–391 (2008)
4. J. Park, Y. Kim, G.T. Kim, J.S. Ha, Adv. Funct. Mater. **21**, 4159–4165 (2011)
5. B.P. Timko, T. Cohen-Karni, G. Yu, Q. Qing, B. Tian, C.M. Lieber, Nano Lett. **9**(2), 914–918 (2009)
6. Z. Fan, J.C. Ho, T. Takahashi, R. Yerushalmi, K. Takei, A.C. Ford, Y.L. Chueh, A. Javey, Adv. Mater. **21**(37), 3730–3743 (2009)
7. T. Hanrath, B.A. Korgel, Proceedings of the institution of mechanical engineers. Part N **218**, 25–34 (2005)
8. B. Dorin, P. Parkinson, P. Scully, J. Mater. Chem. C **5**, 4923–4930 (2017)
9. B.Y. Ahn, E.B. Duoss, M.J. Motala, X. Guo, S.-I. Park, Y. Xiong, J. Yoon, R.G. Nuzzo, J.A. Rogers, J.A. Lewis, Science **323**(5921), 1590–1593 (2009)
10. M. Schumann, R. Sauerbrey, M.C. Smayling, Appl. Phys. Lett. **58**(4), 428–430 (1991)
11. S. Küper, J. Brannon, K. Brannon, Appl. Phys. A **56**, 43–50 (1993)
12. X. Gu, Appl. Phys. Lett. **62**, 1568–1570 (1993)
13. R. Srinivasan, R.R. Hall, W.D. Loehle, W.D. Wilson, D.C. Allbee, J. Appl. Phys. **78**, 4881–4887 (1995)
14. J. Lin, Z. Peng, Y. Liu, F. Ruiz-Zepeda, R. Ye, E.L.G. Samuel, M.J. Yacaman, B.I. Yakobson, J.M. Tour, Nat. Commun. **5**(5714), 1–8 (2014)
15. Z. Peng, R. Ye, J.A. Mann, D. Zakhidov, Y. Li, P.R. Smalley, J. Lin, J.M. Tour, ACS Nano **9**(6), 5868–5875 (2015)
16. J.B. In, B. Hsia, J.H. Yoo, S. Hyun, C. Carraro, R. Maboudian, C.P. Grigoropoulos, Carbon **83**, 144–151 (2015)
17. S. Luo, P.T. Hoang, T. Liu, Carbon **96**, 522–531 (2016)
18. S. Wang, Y. Yu, R. Li, G. Feng, Z. Wu, G. Compagnini, A. Gulino, Z. Feng, A. Hu, Electrochim. Acta **241**, 153–161 (2017)
19. F. Cui, A. Liu. Kingbright Technical Data Sheet (KPHHS-1005SECK) (2013)
20. A. Ferrari, J. Robertson, Phys. Rev. B **61**(20), 14095–14107 (2000)